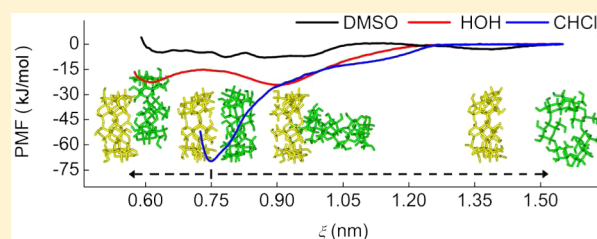


Molecular Recognition in Different Environments: β -Cyclodextrin Dimer Formation in Organic Solvents

Haiyang Zhang,^{†,‡} Tianwei Tan,^{*,†} Wei Feng,[†] and David van der Spoel^{*,‡}[†]Department of Biochemical Engineering, Beijing Key Laboratory of Bioprocess, Beijing University of Chemical Technology, Box 53, 100029 Beijing, China[‡]Department of Cell and Molecular Biology, Science for Life Laboratory, Uppsala University, Husargatan 3, Box 596, SE-751 24 Uppsala, Sweden

Supporting Information

ABSTRACT: Electrostatic and van der Waals interactions as well as entropy contribute to the energetics governing macromolecular complexation in biomolecules. Hydrogen bonds play a particularly important role in such interactions. Here we use molecular dynamics (MD) simulations to investigate the hydrogen bond (HB) orientations of free β -cyclodextrin (β -CD) and head-to-head dimerization of β -CD monomers with and without guest molecules in different environments, namely, in 10 different solvents covering a wide range of polarity. Potentials of mean force for the dimer dissociation are derived from umbrella sampling simulations, allowing determination of the binding affinity between monomers. The HB orientations are in good agreement with available experimental data in water and dimethyl sulfoxide, yielding confidence in the force field used. HB exchanges at the secondary rim of β -CD are observed with a fast rate in water and with a low rate or even no exchange in other solvents. Orientational preferences of interglucopyranose HBs and their effects on the β -CD structure in these solvents are discussed in detail. Polar solvents with stronger HB accepting abilities can interrupt intermolecular HBs more easily, resulting in a less stable dimer. Guest molecules included in the channel-type cavity strengthen the binding affinity between two monomers to some extent, particularly in polar solvents. Formation of the head-to-head dimer is therefore solvent-dependent and guest-modulated. There is only limited correlation between the dimer binding energies and solvent properties like the dielectric constant. This implies that implicit solvent models will not be capable of predicting important properties like binding energy for other solvents than water without a complete reparameterization. This work provides a deeper comprehension on the properties of β -CD, and implications for the application of cyclodextrins in aqueous and nonaqueous media are discussed.



INTRODUCTION

Cyclodextrins (CDs) are a family of cyclic oligosaccharides with six or more D-glucopyranose subunits joined together by α -1,4 glycosidic linkages. α -, β -, and γ -CD are typical CDs composed of six, seven, and eight glucopyranose residues in a ring, respectively, creating a somewhat hydrophobic cavity and a hydrophilic surface.^{1,2} This property allows guest molecules of suitable size to be accommodated in CD cavities and hence leads to a wide range of interesting applications, like in the food industry, in separation science, and pharmaceuticals.^{3–7} CDs have been studied at length not only as excellent hosts for molecular recognition but also as cyclic components for construction of molecular devices.^{8,9} Most frequently, CD/substrate inclusion complexes exist with a host:guest ratio of 1:1, which represents the essence of molecular encapsulation. Stoichiometric ratios of 1:2, 2:1,^{10,11} or an unusual association ratio of 3:2 have been determined as well.¹² In recent years, much attention has been paid to CD-based supramolecular polymers, such as polyrotaxanes with more than four CD units arranged linearly along polymer chains, in order to achieve more sophisticated structures and functions.¹³

By association of two CD units, a dimer is formed with a channel-like cavity. Hydrogen bonding between the two monomers has been suggested to contribute to the dimer stabilization.^{14–17} In the monomeric form, a belt of seven interglucopyranose hydrogen bonds (HBs) at the secondary rim of β -CD was proposed to be responsible for its rigid structure and low solubility in water, relative to α - and γ -CD.^{18–20} An intramolecular interglucopyranose HB can be oriented in two types; type A looks like (2)OH \rightarrow O(3')H (Figure 1a), and type B is H(2)O \leftarrow HO(3') (Figure 1b). When forming a secondary face-to-face dimer, also called head-to-head (HH), the difference in HB orientations leads to two types of dimers. These two structures for the β -CD monomer (MA and MB) and dimer (DA and DB) are shown in Figure 1. The other two possible dimers (not shown here) are head-to-tail (HT) and tail-to-tail (TT); head indicates the secondary rim and tail the primary rim.

Received: July 7, 2012

Published: October 1, 2012

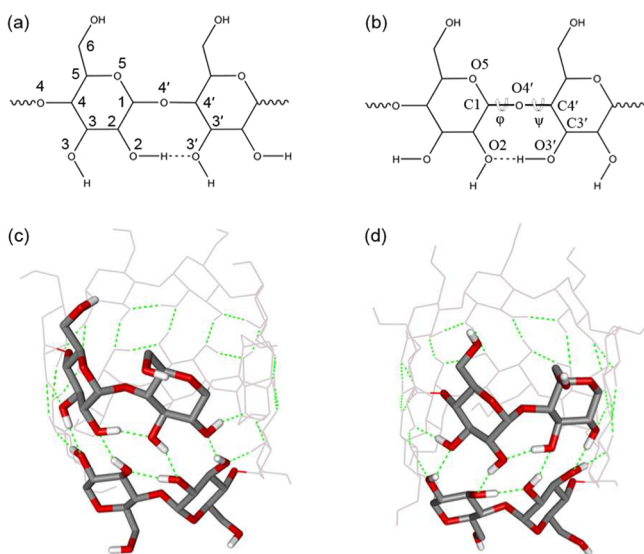


Figure 1. Two orientations of interglucopyranose hydrogen bonds (HBs) (a, b) and two types of β -CD dimers with 14 complementary intermolecular HBs (c, d). Two glucopyranose residues are marked by the atom index and name (a, b). φ and ψ are two dihedral angles at the bridging oxygen atoms (b). Interglucopyranose HBs at the secondary rim of CDs can be oriented in two fashions; type A (a) is $(2)\text{OH} \rightarrow \text{O}(3')\text{H}$ and type B (b) $\text{H}(2)\text{O} \leftarrow \text{HO}(3')$, where the single prime indicates an adjacent glucopyranose and the arrow points to the acceptor oxygen. The β -CD dimer formed by two monomers with A-type HBs is denoted as dimer DA (c); dimer DB (d) for B-type.

So far, there are few studies related to the HB orientations of CDs and the binding between two monomers, although the cooperative binding of the CD dimer to guest molecules is well-known. Harada et al. reported an X-ray diffraction study on rotaxane structures between α -CD and poly(ethylene glycol) (PEG) where the PEG chain is included in a channel formed by association of α -CDs in HH and TT orientations.²¹ A theoretical explanation for α -CD-PEG polyrotaxanes using molecular dynamics (MD) was reported by Mattice's group who indicated that HBs between successive α -CDs slightly prefer HH and TT sequences over HT.¹⁶ Quantum chemical calculations on α -CD dimers embedded in a water cluster revealed that the HH mode is preferred over HT and TT. When water tetramers are trapped between two α -CD monomers, HH is destabilized and TT stabilized.²² Another set of quantum calculations showed that the β -CD monomer MA is energetically more favorable than MB and that the HH dimer DB is preferred over DA, due to the geometric preference and the difference in HB orientations.¹⁴ However, MD simulations with the Amber force field indicated that HH is the most stable for β -CD dimers *in vacuo* due to the existence of 14 complementary intermolecular HBs,¹⁵ while in water TT is predicted to be more stable.²³ In a very recent report, Tallury et al. simulated different orientations of β -CD rings on a single polyaniline chain using molecular dynamics with an implicit solvent model and concluded that β -CD monomers tend to be more attractive in the HT configuration and more repulsive in HH, a result affected by the choice of the dielectric constant.²⁴

Molecular dynamics (MD) simulation is perhaps the most direct way to theoretically explore the molecular behavior that may not be accessible to experimental approaches. Many groups have performed MD simulations to investigate free CDs and CD-based complexes and contributed valuable explanations

for the molecular mechanisms behind experimental observations.^{11,18,20,24–30} An especially useful method in analyzing molecular complexation is umbrella sampling.^{31–33} This method has been applied, among many things, to investigate protein–ligand binding and peptide dissociation,^{34,35} solute permeation into lipid membranes,^{36,37} CD-shuttling in molecular switches,³⁸ and solvation of ions and organic molecules in water droplets.^{39,40} For details on umbrella sampling simulations, we refer to these reports.^{34–40} Another technique, center-of-mass (COM) pulling or steered molecular dynamics (SMD), allows one to explore processes on the time scale accessible to conventional MD, like unbinding of ligands,³⁵ and provides an effective approach to generate a number of configurations for umbrella sampling simulations.

Here we present an extensive molecular dynamics study on the free β -CD monomer and on the dimer with and without guest in a series of common solvents ranging from polar to nonpolar. HB orientations in the monomer and dimer are taken into account as well. β -CD dimers containing guest molecules are most often crystallized in a HH orientation, and only the HH dimer is therefore considered in this work. The guest molecule umbelliferone forms a 2:2 inclusion complex with the dimer studied in the crystal structure.⁴¹ COM pulling simulations are performed to generate a dissociation pathway of the dimer with and without guest, and then, we employ the umbrella sampling technique to compute potentials of mean force (PMFs) for the dimer dissociation, allowing the binding affinity between the two monomers to be determined. Since this work addresses HB orientations and the dimer stability with and without guest molecules in polar and nonpolar solvents, it provides implications for the CD-based supra-molecular mechanisms underlying molecular recognition.

METHODS

Structural Model. The initial structure of a head-to-head β -CD dimer was taken from the Cambridge Crystallographic Data Centre (CCDC no. 785103) where the dimer forms a 2:2 complex with two umbelliferone molecules.⁴¹ Umbelliferone has been reported to exhibit a wide range of bioactivities.⁴² Two HB fashions of type A and type B for the β -CD monomer and dimer (Figure 1) were obtained with the aid of the Discovery Studio Visualizer and Chem3D software. Interestingly, the former gives β -CD hydrogen atoms in the fashion of type A, whereas the latter chooses type B. More details are given in the Supporting Information.

Simulation Protocol. The q4md-CD force field⁴³ was selected to model CDs. This force field is a combination of GLYCAM04^{44–46} and Amber99SB⁴⁷ and has been reported to have good performances toward CDs using the Amber 10 software⁴⁸ in a recent paper.⁴³ Here we have validated its performance with the GROMACS suite^{49,50} for solvated α -, β -, and γ -CD monomers in water (see the validation in the Supporting Information). The generalized Amber force field (GAFF)⁵¹ was used for methanol (MeOH), ethanol (EtOH), dimethyl sulfoxide (DMSO), *N,N*-dimethylacetamide (DMA), *N,N*-dimethylformamide (DMF), acetone (ACO), tetrahydrofuran (THF), acetonitrile (ACN), and chloroform (CHCl_3). Their equilibrated liquid structures and topology files were taken from the GROMACS Molecule & Liquid database,⁵² available online at <http://virtualchemistry.org/>. Details on how the database was generated, as well as the derivation of atomic charges for these solvent molecules, were recently published by Coleman et al.⁵³ The guest molecule umbelliferone was also

parametrized by the GAFF force field with the restrained electrostatic potential charges.⁵⁴ Note that scaling factors for 1–4 nonbonded interactions and charge derivations in the q4md-CD force field and GROMACS Molecule & Liquid database both follow the Amber scheme, which ensures consistency and compatibility between these parameters. As an Amber-like force field, the q4md-CD should be compatible to organic media that are parametrized by the GAFF. The three-point transferable intermolecular potential (TIP3P)⁵⁵ was used to model water. The default factors of 1/2 and 1/1.2 for the Amber all-atom potential⁵⁶ were applied to scale 1–4 Lennard-Jones and electrostatic interactions, respectively. All the simulations were carried out using the GROMACS suite,^{49,50} version 4.5.5, at 300 K and 1 bar. More details on the simulation protocol have been presented in ref 57.

Normal Simulation. The β -CD monomers (MA and MB) were separately immersed in a pure liquid of 10 solvents listed in Table 1. Each case for one monomer (20 in total) was run 10

Table 1. Property of Solvent Molecules Studied

| solvent | HBD ^a | HBA ^a | log P^b | D^c |
|-------------------|------------------|------------------|-----------|-------|
| HOH | 0.82 | 0.35 | | 80 |
| MeOH | 0.43 | 0.47 | −0.77 | 33 |
| EtOH | 0.37 | 0.48 | −0.31 | 25 |
| DMSO | 0.00 | 0.78 | −1.35 | 47 |
| DMA | 0.00 | 0.78 | −0.77 | 39 |
| DMF | 0.00 | 0.74 | −1.01 | 38 |
| ACO | 0.04 | 0.49 | −0.24 | 20 |
| THF | 0.00 | 0.48 | 0.46 | 8 |
| ACN | 0.07 | 0.32 | −0.34 | 36 |
| CHCl ₃ | 0.15 | 0.02 | 1.97 | 5 |

^aHydrogen bond donor (HBD) and acceptor (HBA) values taken from ref 61. ^b P , n-octanol/water partition coefficients calculated by ALOGPs 2.1.^{63,64} ^cDielectric constant at room temperature.

times with different initial velocities generated from a Maxwell distribution at 300 K with a random seed. All systems were placed in a truncated octahedron box with an image distance of 5 nm. HBs were determined from simulation trajectories using a geometrical criterion based on cut-offs with a donor–acceptor distance of at most 0.35 nm and an acceptor–donor–hydrogen angle of at most 30°.⁵⁸

Umbrella Sampling Simulation. The β -CD dimer was oriented to make the cavity axis parallel to the Z-axis. The COM distance between two monomers along the Z-axis is defined as a reaction coordinate ξ (Figure 2). The pull code in GROMACS^{49,50} was used to generate from a dissociation process of the dimer snapshots for umbrella sampling simulations. Position restraints were imposed on seven glycosidic oxygen atoms of one monomer (called chain A); chain A was used as an immobile reference for pulling simulations. The other monomer (called chain B) was pulled away from chain A along the Z-axis over 1 ns with a harmonic force constant of 1000 kJ mol^{−1} nm^{−2} and a pull rate of 0.001 nm ps^{−1}. A final COM distance of approximately 1.75 nm between chain A and chain B was achieved. Along the reaction coordinate, approximately 40 windows were selected in the range 0.60 nm $\leq \xi \leq$ 1.60 nm with a distance of 0.025 nm between adjacent positions. Values of the mean force were computed within each window, and reassembling all the values from adjacent windows produced a continuous PMF curve as a function of the reaction coordinate. Following the same

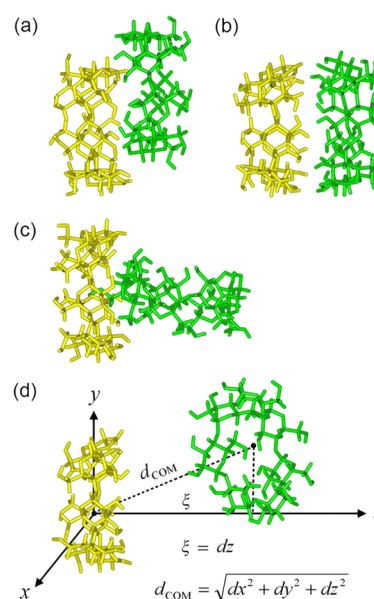


Figure 2. Representative configurations (a–d) during dissociation of β -CD dimer and definition of the reaction coordinate ξ (d). Positions of the snapshots are at $\xi =$ (a) 0.60, (b) 0.75, (c) 0.90, and (d) 1.55 nm. Two monomers are denoted as chain A (in yellow) and chain B (in green). Chain A is used as a reference to define ξ . (b) represents the crystal structure. A path of the dimer dissociation is like a process from (b) to (c) to (d). If not stable, the dimer would shift to state (a) when chain B approaches toward chain A.

approach, two dimers (DA and DB) were simulated in pure liquids of 10 solvents. With guest molecules, only the dissociation of dimer DB was considered because this crystal structure favored 14 complementary intermolecular HBs. The 2:2 complex was simulated in 10 solvents, whereas the 2:1 complex was studied in water only. A total of 31 PMF profiles were therefore obtained. The overall simulation time for a single PMF profile is about 400 ns (10 ns for each window). After removing the first 2 ns for equilibration, the PMFs were constructed with the weighted histogram analysis method (WHAM).^{59,60} Statistical uncertainties of the PMFs were estimated using Bayesian bootstrapping of complete histograms.⁶⁰

RESULTS

Monomer. Considering the importance of HBs in CDs, we chose 10 solvents with different HB propensities as listed in Table 1. Scales of hydrogen bond acidity and basicity were constructed by Abraham,⁶¹ using formation constants of HBs in tetrachloromethane. The scale of solvent hydrogen bond donor (HBD) acidities or hydrogen bond acceptor (HBA) basicities describes the ability of the solvent to donate or accept a proton in a solvent-to-solute hydrogen bond, respectively.^{61,62} The first three solvents (HOH, MeOH, and EtOH) in Table 1 possess both HB accepting and donating properties. Water, with a relatively small HBA value on this scale, is a strong donor. MeOH and EtOH both have similar HBD and HBA values. The last seven molecules with only HB accepting property are sorted by the HBA value in descending order. For these solvents, n-octanol/water partition coefficients^{63,64} (log P values) and dielectric constants are given in Table 1 as well. DMSO, DMA, and DMF with higher HBA values are common

polar solvents and typical HB acceptors. CHCl_3 has a higher log P value and almost no ability to form HBs.

Figure 3a shows the occupancy of interglucopyranose HBs in the 10 solvents. Water (HOH) and DMSO can easily interrupt

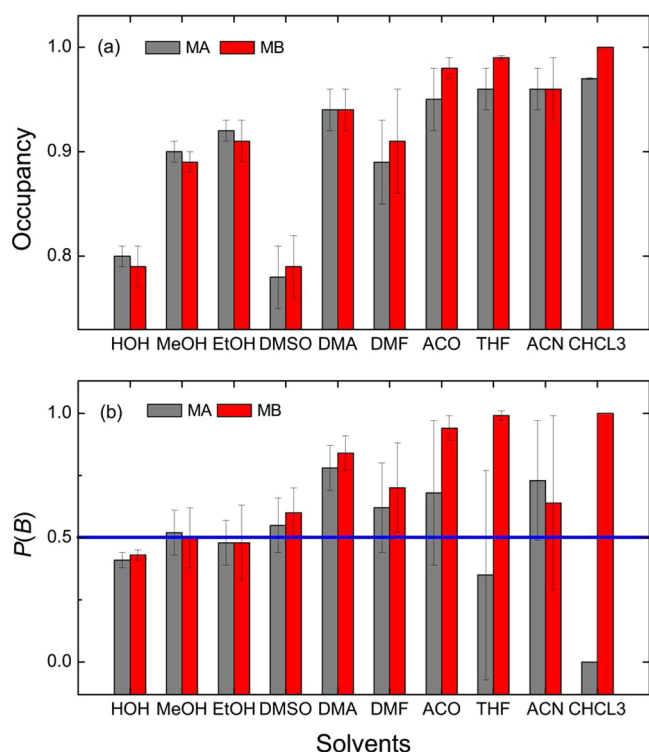


Figure 3. (a) Occupancy of interglucopyranose HBs at the secondary rim of β -CD and (b) probability of the interglucopyranose HB in the fashion of B-type $\text{H}(2)\text{O} \leftarrow \text{HO}(3')$. The occupancy is defined as n_t/n_m , where n_t and n_m are the total number of HBs formed in the simulation and its maximum value of seven between seven interglucopyranose residues, respectively. The probability of A-type $P(A)$ and B-type $P(B)$ is calculated using a formula $P(A) = n_A/n_t = (n_t - n_B)/n_t = 1 - P(B)$, with n_A and n_B being the number of interglucopyranose HBs in the fashion of A-type and B-type, respectively.

HBs and give a low occupancy of approximately 0.8. The occupancy in MeOH and EtOH is about 0.9. DMF behaves similarly to MeOH and EtOH but displays a larger fluctuation. Unexpectedly, DMA with a higher HBA value shows a higher occupancy of 0.94. In the other solvents with lower HBA values, almost all seven interglucopyranose HBs are formed with an occupancy higher than 0.95. There are no significant differences in occupancy for monomer MA and MB in HOH, MeOH, EtOH, DMSO, DMA, DMF, and ACN. For monomer MB in ACO, THF, and CHCl_3 , however, the occupancy even approaches unity, which is higher than for monomer MA.

A neutron diffraction study by Betzel et al.⁶⁵ indicated that secondary hydroxyls are engaged in a flip-flop phenomenon, that is, the HB between two hydroxyls flips from one fashion to the other, and vice versa. Figure 3b presents the probability that the interglucopyranose HB between two adjacent glucopyranoses is in the fashion of B-type $\text{H}(2)\text{O} \leftarrow \text{HO}(3')$ if it exists. The probability of type B in HOH is less than 0.5, indicating a less favorable type B, compared to A-type $(2)\text{OH} \rightarrow \text{O}(3')\text{H}$. In MeOH and EtOH, both fashions of HBs are balanced with a probability of 0.5. In DMSO, DMA, DMF, ACO, THF, and

ACN, type B is preferred. During the simulations in ACO and THF, there are almost no switches from type B to type A for monomer MB. However, HB orientations for monomer MB can be more easily exchanged between type A and type B in ACN than in ACO and THF. Larger errors are observed for monomer MA in ACO and THF and for monomer MA and MB in ACN because the HB orientation does not easily switch once it changes from one fashion to the other in these solvents. In CHCl_3 , initial orientations of HBs for monomer MA and MB persist throughout MD simulations, and no exchange is detected between type A and type B.

Figure 4 describes a dynamic exchange of HBs between one pair of secondary hydroxyls along the simulation time. HB

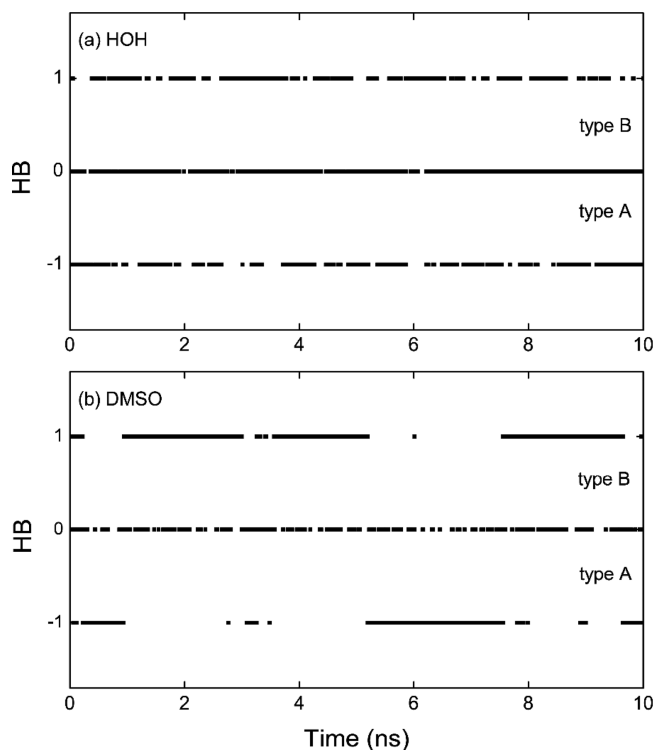


Figure 4. Dynamics of hydrogen bond exchanges, called flip-flop, between one pair of hydroxyl groups belonging to adjacent glucopyranose residues in (a) HOH and (b) DMSO during a 10 ns simulation. The value 1 means type B and -1 for type A.

orientations frequently exchange between type A and type B in HOH (Figure 4a). The exchange in DMSO is observed with a lower rate (Figure 4b). The flip-flop mechanism of HBs can also be detected in MeOH, EtOH, DMA, and DMF, with a lower rate than in water (not shown here). For monomer MA in ACO and THF and for monomer MA and MB in ACN, one fashion can exist for a long time until it changes to the other and a very slow flip-flop occurs during the simulation. These findings are consistent with the notion that the enthalpy of activation for breaking HBs is considerably higher in a hydrophobic environment than in a hydrophilic one.⁶⁶

Flip-flops can affect the mobility of hydrogen atoms involved in the hydrogen bonding or even put pressure on the entire structure. Root-mean-square fluctuations (RMSFs) of β -CD from the crystal structure, which pinpoint individual atomic fluctuations, are calculated with mass weighting and presented in Figure 5. To identify different atoms, one glucopyranose residue is shown in Figure 5a with atom indexes and names. β -

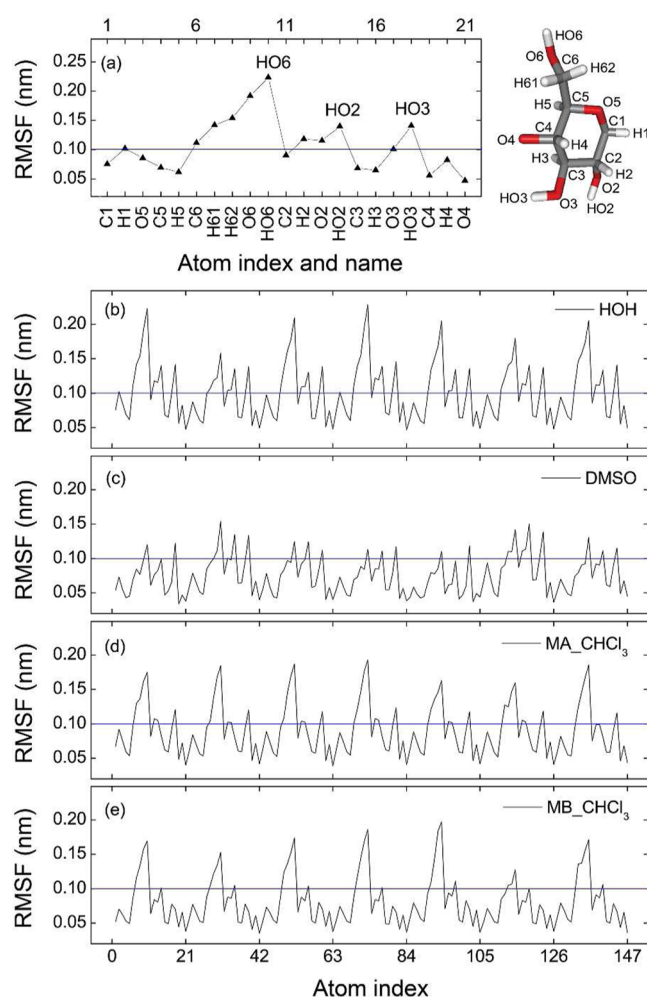


Figure 5. Root-mean-square fluctuation (RMSF) of atomic positions from the crystal structure for one glucopyranose residue (a), for β -CD in pure (b) HOH and (c) DMSO, and for (d) monomer MA and (e) monomer MB in CHCl_3 . MA and MB in HOH and DMSO show similar RMSFs. The blue line indicates 0.1 nm for the RMSF. Each glucopyranose contains 21 atoms, and the RMSF of one glucopyranose (a) is taken from the first residue of β -CD in HOH (b).

CD displays larger fluctuations in HOH than in DMSO and CHCl_3 . Hydrogen atoms (HO6) of primary hydroxyls are more flexible than secondary ones (HO2 and HO3). The mobility of primary hydroxyls in these three solvents is in the order of $\text{HOH} > \text{CHCl}_3 > \text{DMSO}$. The HO2 and HO3 atoms have a very similar flexibility in HOH (Figure 5b). In DMSO, HO3 is more flexible than HO2 in some glucopyranose residues, but the picture is opposite in other ones (Figure 5c). In CHCl_3 , the HO3 atoms bear larger fluctuations than HO2 for monomer MA (Figure 5d), whereas they show smaller fluctuations than HO2 for monomer MB (Figure 5e).

Dimer without Guest. Figure 6 presents the PMFs for the dissociation of dimers DA and DB along the reaction coordinate ξ . Figure 2 shows representative configurations along the reaction coordinate. The first three, at 0.60 nm (Figure 2a), 0.75 nm (Figure 2b), and 0.90 nm (Figure 2c), are similar to the layer-, channel-, and cage-types of crystal packing patterns of CDs, respectively.^{67,68} The channel-type (Figure 2b) was used as the initial coordinate for pulling simulations to generate the dissociation process of the dimer. At 1.55 nm, two

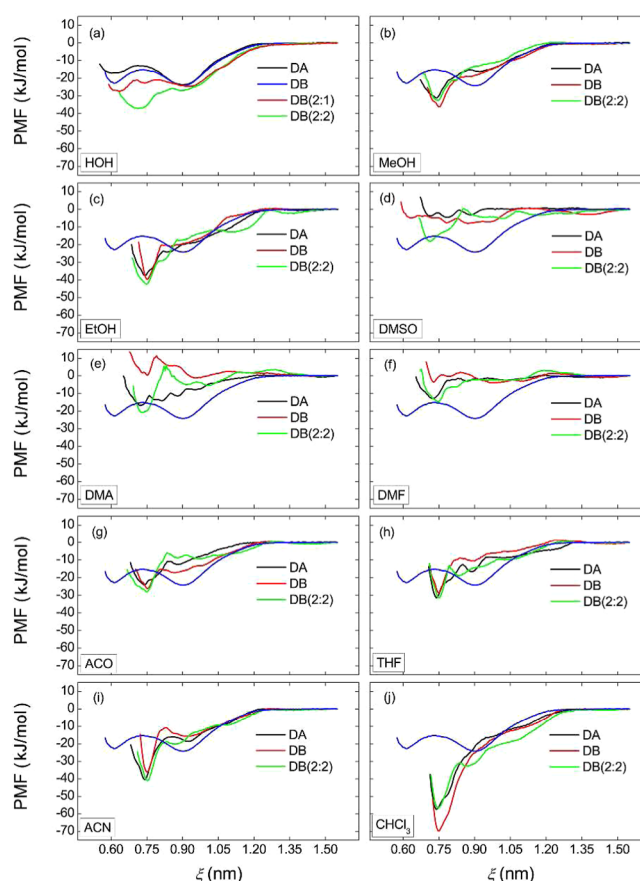


Figure 6. Potentials of mean force (PMFs) for dimers DA and DB, and for the dimer DB with guest molecules in 10 solvents. DB(2:1) indicates a complex of the dimer DB with one guest and DB(2:2) for two guest molecules. The PMF for DB in HOH, indicated by a blue line, is shown in each solvent for comparison. Error bars are less than 4 kJ/mol and not given here for clarity.

monomers are completely separated from each other (Figure 2d) and there is no interaction between them.

All PMFs are defined to zero at 1.55 nm in the reaction coordinate, and thus, the minima of the PMFs quantify the free energy difference with respect to the separated state of two monomers. The PMF profile for dimer DB in water, indicated by a blue line, is shown in all the solvents for comparison. As shown in Figure 6, all the PMFs approach zero and level off in the range $\xi \geq 1.35$ nm, corresponding to the separated state of two monomers. In water, two minima at approximately 0.60 and 0.90 nm are observed for dimers DA and DB (Figure 6a), indicating that the channel-type is not stable and that the dimer tends to form layer- or cage-type structures. In DMSO, two monomers are weakly bound together with a binding free energy close to zero (Figure 6d). DMA and DMF also give a weaker binding than HOH, and there seems to exist a large difference in the binding for dimer DA and DB (Figure 6e and f). In MeOH (Figure 6b), EtOH (Figure 6c), ACO (Figure 6g), THF (Figure 6h), ACN (Figure 6i), and CHCl_3 (Figure 6j), the dimers can maintain a channel-type structure somewhat and are more stable than in other solvents. MeOH and EtOH both give a larger binding free energy than THF, and the binding for EtOH is slightly stronger than for MeOH. For the solvents with only HB accepting property and lower HBA values, a smaller HBA value corresponds to stronger binding, that is, $\text{ACN} > \text{THF} > \text{ACO}$. CHCl_3 , which can neither accept

nor donate HBs, induces a very strong binding between monomers (Figure 6j).

Dimer with Guest. The PMFs for dimer DB with guest are computed and also shown in Figure 6 for comparison. As shown in Figure 6a, one guest increases the stability of dimer DB, indicated by the red line for DB(2:1), and a local minimum is observed near 0.75 nm, where the dimer adopts the channel-type structure. For the two guest molecules included, the stability of dimer DB is further strengthened with a binding free energy of 37 kJ/mol, indicated by the green line for DB(2:2). Moreover, the PMF displays a wider profile near 0.75 nm, which means the channel-type dimer still tends to be in a layer- or cage-type fashion. Snapshots of 2:1 and 2:2 complexes during the simulation in water are given in Figure 7. For one

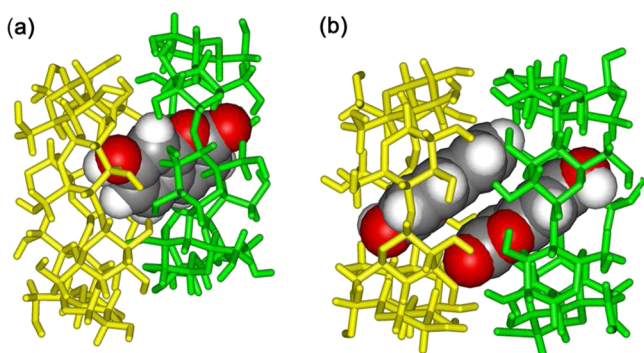


Figure 7. Snapshot of the dimer DB with (a) one guest and (b) two guests, representing the states of approximately 0.60 and 0.75 nm in the reaction coordinate, respectively. Guest molecules (umbelliferone) are shown with space-filling models.

guest, the channel-type dimer cannot be maintained easily and a layer-type arrangement is preferred (Figure 7a). In the 2:2 complex, two guests reside parallel within the channel cavity with their lactone rings facing each other (Figure 7b). Although dimer binding in DMSO, DMA, and DMF is strengthened by guest molecules (Figure 6d–f), it is still weaker than in other solvents (Figure 6). In water, two guests give a significant increase in the binding affinity of two monomers (Figure 6a). No obvious enhancements on the dimer stability are observed in MeOH, EtOH, ACO, THF, and ACN when two guests are included in the dimer cavity. Unexpectedly, inclusion of guests weakens the binding between two monomers in CHCl_3 , although a strong binding still exists.

Correlation of Dimer Binding Energy with Solvent Properties. In order to evaluate the predictive power of the solvent properties in Table 1, we have plotted the channel-type dimer binding energies of the CDs in DA and DB configuration, as well as the (2:2) host–guest complex, as a function of these properties (Figure 8). The $\log P$ and HBA correlate reasonably well with the binding energy ($R^2 \approx 0.7$ – 0.9); however, if we leave out one point, for solvation in chloroform, the correlation drops significantly. HBD does not correlate to the binding free energy at all (Figure 8c). Since the electrostatic energy of dipole molecules in different media was estimated to vary as a formula $2(D - 1)/(2D + 1)$, where D is the dielectric constant,^{69,70} we used this formula to correlate to the binding energy. Dielectric constants correlate only weakly to the dimer binding ($R^2 \approx 0.4$ – 0.5) (Figure 8d). Note that solute polarization and solvation entropy upon association of monomers may contribute to the dimer binding as well and

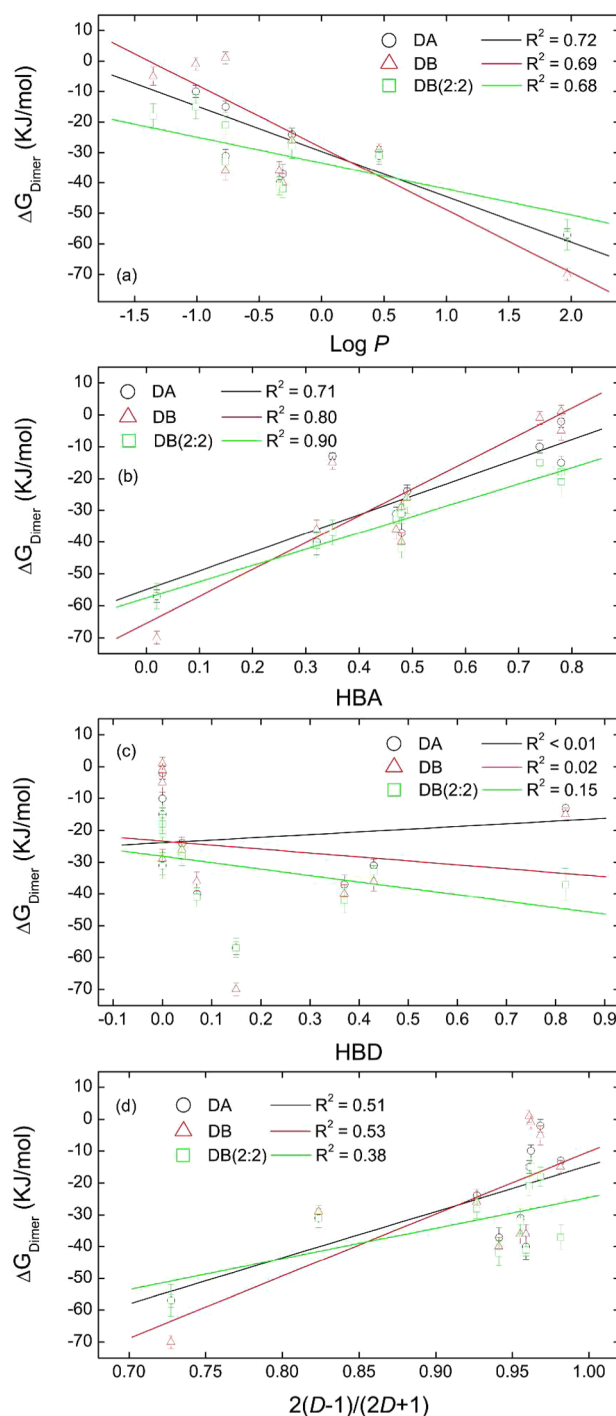


Figure 8. Binding free energy (at $\xi = 0.75$ nm) of monomers in the channel-type dimer DA (black), DB (red), and (2:2) complex (green) versus solvent properties of (a) polarity ($\log P$), (b) hydrogen bond acceptor (HBA) value, (c) HB donor (HBD) value, and (d) $2(D - 1)/(2D + 1)$, where D is a dielectric constant. For each dimer, a linear fit to data points is plotted in the same color and R^2 is the correlation coefficient.

they are not expected to behave linearly. Obviously, the binding energy is a complex function of the interacting molecules and the environment (solvent) and simplifications based on solvent properties like the dielectric constant cannot on their own predict the binding energy.

DISCUSSION

Flip-flops with participation of water molecules have been confirmed for all natural CDs by the neutron diffraction technique.⁴³ Solvent molecules may interrupt HBs and help to form new ones. Given that an interglucopyranose HB can assist in keeping rigid—to some extent—the structure of two adjacent glucopyranoses that are involved in the hydrogen bonding, one pair of HBs with a rapid exchange would on average act on both glucopyranoses and hence maintain a rigid structure. The RMSF plots (Figure 5) show that the rapid exchange of HBs in water endows β -CD with a large fluctuation in structure while keeping the overall structure. The HB with a slow exchange rate affects the spatial arrangement of glucopyranose residues in a particular direction and may cause a structural deformation, as shown in Figure 5b for β -CD in DMSO where the second and sixth glucopyranose residues show larger fluctuations than others. In DMSO, DMA, and DMF, type B is preferred (Figure 3b) and HB exchanges are slower than in water. β -CD displays structural deformations in these solvents; for instance, the tilting of glucopyranose residues swings with a large deviation, either inward or outward with respect to the cavity, similar to what was discussed in previous reports.^{57,71}

A belt of seven interglucopyranose HBs with no exchange in CHCl_3 helps β -CD to maintain its rigidity, but it leads to a more strained structure compared to that in water and the monomer MA is more strained than MB. Smaller fluctuations are observed for the bridging oxygen atoms (named O4 in Figure 5) in CHCl_3 than in water (Figure 5 and Figure S2 in the Supporting Information), indicating a more rigid cavity in CHCl_3 . Two dihedral angles φ and ψ (Figure 1b) at the bridging oxygen atoms can be used to evaluate conformational torsions in CDs.¹⁴ As shown in Figure S3 in the Supporting Information, the distribution of φ shifts to bigger values in CHCl_3 compared to that in HOH and the shift for MA is larger than MB. For ψ , the distribution slightly shifts to smaller values in CHCl_3 and no significant difference is observed for MA and MB. These findings in CHCl_3 are in good agreement with quantum calculations of β -CD in the gas phase.¹⁴

Due to the directionality of HBs, the fashion of A-type (2)OH \rightarrow O(3')H may limit movement of the hydrogen HO2, whereas the other hydrogen HO3' is more flexible. Similarly, HO2 is more flexible for type B. As expected, the mobility of hydrogen atoms for monomer MA and MB in CH_3Cl_3 follows this rule, as shown in Figure 5d,e. However, HO2 and H3O in water bear very similar fluctuations due to fast exchanges, although type A is preferred (Figure 3b). For HB exchanges with a low rate, like in DMSO (Figure 4b), it is hard to correlate HB orientations with the hydrogen flexibility (Figure 5c). According to the fluctuations of HO2 and HO3 in Figure 5, HO2 seems inherently more flexible than HO3.

Intermolecular HB-exchanges between CDs and water cannot be detected by NMR experiments, due to the fast exchange beyond the NMR time scale. NMR studies on flip-flop HBs of CDs in DMSO indicated that type B is predominant and the mobilities of hydroxylic protons are on the order of $\text{HO6} > \text{HO2} > \text{HO3}$.^{72,73} In our simulations, we observe a more favorable type B (Figure 3b) and a slower HB exchange in DMSO (Figure 4b). Type B may increase the flexibility of the HO2 atom, and the slow exchange rate may facilitate the NMR measurement. To our knowledge, there are no experimental data available to compare with MD results in

the other solvents studied. Similar to β -CD, type A is preferred over type B for α -CD in water (see Table S1 in the Supporting Information), which is consistent with *ab initio* calculations on conformers of α -CD by Anconi et al. who evaluated thermal correction and solvation energy contributions and reported that the HB fashion of type A is more favorable in the gas phase and aqueous media.⁷⁴ These NMR experimental and quantum chemical results strongly suggest that our calculations are correct.

Three types of hydroxyl groups of CDs have different reactivity.⁷⁵ The (6)OH groups, being primary alcohols, are more nucleophilic than (2)OH and (3)OH which are secondary alcohols. The different role in the belt of interglucopyranose HBs gives different reactivities for (2)OH and (3)OH. On the basis of temperature-dependent NMR studies in DMSO,⁷² (3)OH is the predominant proton donor, that is, type B is preferred, and hence, (2)OH is more acidic than (3)OH.⁷⁵ The difference in reactivity can be used to selectively synthesize cyclodextrin derivatives in which the hydroxyls of one, two, or three types are modified.⁷⁵ Casu and co-workers⁷⁶ reported a resistance to methylation of (3)OH for α - and β -CD with dimethyl sulfate in a mixture of DMSO and DMF, and inferred that hydrogen bonding in the fashion of B-type $\text{H}(2)\text{O} \leftarrow \text{HO}(3')$ protected the (3)OH group somewhat. If so, fast HB-exchanges would go against CD modifications at the C2- and C3- positions, which may be a reason why water is not an ideal solvent for this kind of reactions, the low solubility of CDs in water forming another problem. Actually, CD modifications at the secondary rim are often prepared in a buffer containing polar solvents like DMSO and DMF.^{75,77–80} In our simulations, type B is more favorable and HB exchanges are relatively slow in DMSO, DMA, and DMF. These observations may facilitate CD modifications at the C2-position and provide implications for CD-containing reactions in polar solvents.

An explanation for preferred HB orientations can be deduced from the acidity of (2)OH groups and from HB properties of organic solvents studied. The more acidic (2)OH group endows it with a strong HB donor, and the O(2) atom has a larger electronegativity than O(3); that is, (2)OH groups are better proton donors than (3)OH in the HB formation. Actually, the atomic charges used in our simulations for O(2), HO2, O(3), and HO3 are -0.635 , 0.437 , -0.620 , and 0.422 *e*, respectively.⁴³ As expected, type A (2)OH \rightarrow O(3')H is more stable for the monomer. In the HH dimer, type B is formed, leaving the (2)OH group as a donor to hydrogen bond to the other monomer. This explains the finding that the dimer DB is more stable than DA. Water is a strong donor and prefers to hydrogen bond to the O(2) atom rather than O(3), due to the difference in electronegativity. This preference does not affect type A, and hence, type A is more favorable in water. However, the solvent with only the HB accepting property prefers to look for a strong donor and probably competes with O(3) for hydrogen bonding to (2)OH, which affects the fashion of type A. Therefore, type B seems to be the dominant state for β -CD in DMSO, DMA, DMF, ACO, THF, and ACN. MeOH and EtOH possess similar HBA and HBD properties (Table 1) and hence give a balance between two fashions with a probability of 0.5 (Figure 3b).

From our PMF calculations in water, the layer- and cage-type have a stronger binding between two monomers than the channel-type, and the cage-type appears more stable than the layer-type (Figure 6a); that is, the channel-type prefers to be in

the pattern of layer- or cage-type, which is in good agreement with a report by Bonnet and co-workers.²³ Including one nonpolar guest molecule (umbelliferone) in the channel cavity increases the dimer stability to some extent (Figure 6a), due to host–guest interactions. Being a small guest, however, one umbelliferone molecule cannot fill two hydrophobic cavities effectively (Figure 7a) and hence the dimer tends to shift to the layer- or cage-type. When two umbelliferone molecules are included, the channel cavity is effectively occupied by the guest molecules (Figure 7b), yielding a stable channel-type dimer, like in the crystal structure. Most of the applications of CD molecules take place in aqueous solution, and the β -CD dimer is often crystallized in the HH channel-type orientation, containing one or two guest molecules.^{10,12,41,81} Harata and Kawanno⁸² crystallized a 2:1 complex of α -CD with isosorbide dinitrate, which is also a HH channel-type structure but with a displacement between two monomers, similar to the layer-type. They reported that the guest modulated the dimer to attain the most stable accommodation into the cavity. We therefore come to the conclusion that formation of CD dimers (like channel-type) is guest-driven and also guest-modulated.

Cyclodextrin inclusion complexes crystallize in three main different patterns, the layer-, channel-, and cage-type,^{67,68} similar to what we observed in Figure 2. Displacement of the channel-type produces the layer-type, similar to Figures 2a and 7a, and the cage-type in most cases prevents one cavity from hosting another molecule. CDs have been reported to exist in solution as aggregates held together by intermolecular hydrogen bonding and bridging water molecules, and aggregation contributes to their low solubility.⁸³ On the basis of our calculations in water, the layer- and cage-type are more stable than the channel-type (Figure 6a). The CD aggregates are probably arranged in one of the three patterns. MD simulations by Anconi et al. reported a quite stable aggregate of three α -CD monomers where the individual molecules are assembled in a perpendicular arrangement to its neighbors,⁸⁴ similar to the cage-type (Figure 2c) in our calculations. Disordered aggregates (like layer- and cage-type) can shield CD cavities to some extent and should be avoided for effective utilization of the cooperative effect of two hydrophobic cavities.

In polar solvents, like DMSO, DMF, and DMA, a weak dimer binding is observed. Even if two guests are included in the channel cavity, the channel-type dimer is still less stable than in other solvents. This instability can be ascribed to the strong HB accepting ability of these solvents and to the electrostatic repulsion between two monomers. These solvents have a higher ability to interrupt (intra- and intermolecular) interglucopyranose HBs and produce an exchange of HBs with participation of solvents. When solvent molecules compete with the two monomers for hydrogen bonding to secondary hydroxyls of CDs, the network of complementary HBs would be destroyed somewhat and the dimer therefore destabilized. Moreover, the HB exchange may increase the probability of the contact of like charges, causing repulsion between two monomers. The repulsion may lead to a displacement between two monomers and even to a partial dissociation of the dimer. As shown in Figure S4 in the Supporting Information, electrostatic interactions between the two monomers are weaker in HOH and DMSO compared to that in the solvents with lower HBA values. In order to avoid the electrostatic repulsion, CD dimers give up the channel-type structure and prefer layer-type arrangements. In this manner, two monomers may come closer together, like in Figure 2a. Tallury et al. placed

β -CD monomers on a single polyaniline chain using implicit solvent models and concluded that the monomers in the HH mode remain closer together in a higher dielectric medium; that is, the repulsion between monomers is weakened as the dielectric increases.²⁴ In this work, we use explicit solvent models with dielectric constants varying from 5 to 80 (Table 1), since details of hydrogen bonding are difficult to discern using implicit solvent models. However, only a limited correlation between the dimer binding and dielectric constants is observed (Figure 8d). Unlike DMA, MeOH, being a common polar solvent with a similar polarity to DMA, gives a stronger binding, which may be due to its relatively small HBA and HBD values not capable of effectively interrupting intermolecular HBs between two monomers.

In solvents with lower polarities, like ACO, THF, and ACN, the HBs exchange at a very low rate and in some cases no exchange is observed. Although not all the 14 complementary intermolecular HBs are occupied during the simulation, these solvents with a lower HBA value cannot effectively interrupt HBs like polar solvents with a higher HBA do. The slow HB-exchange does not facilitate effective interactions between like charges. A stronger electrostatic interaction between two monomers is detected in these solvents (Figure S4 in the Supporting Information). Therefore, a stronger dimer binding is observed in these three solvents. Figure S4 also shows that stronger electrostatic interactions exist between monomers in dimer DA than in DB, which explains the fact that the PMFs for dimer DA extend to the region of smaller values in the reaction coordinate. In CHCl_3 , the two monomers show a very strong binding strength and the dimer DB is more stable than DA, due to the geometric preference and the strong HB network. As indicated by quantum calculations in the gas phase,¹⁴ type A is preferred over type B in the monomeric form, whereas the HB network in dimer DB is stronger than in DA. For dimer DB, it contains two less strained monomers and has stronger intermolecular HBs, so DB is energetically more favorable. During our simulations in CHCl_3 , a less strained MB is also observed (mentioned above). Thus, the binding for the dimer DB without guests in CHCl_3 is obviously stronger than DA (Figure 6j). Including two guest molecules does not lead to a significant increase in the dimer binding in ACO, THF, and ACN but to a decrease in CHCl_3 . CD–guest interactions may affect the macrocycle structure somewhat, as noted by previous reports.^{57,85} If so, the guest included in the dimer DB may induce a conformational change in the CD structure and modulate the dimer binding. In CHCl_3 , for instance, the β -CD cavity is more compressed or stretched upon the guest binding compared to that without guests, as shown in the Supporting Information.

Due to the structural flexibility, it is very hard to determine which dimer is energetically more favorable from our umbrella sampling simulations, except for the dimer in CHCl_3 where the intra- and intermolecular HBs almost do not exchange between type A and type B. Moreover, if a slight displacement between two monomers in the channel-type dimer occurs, should this structure be defined to be layer-type or still be channel-type? Maybe this displacement does lead to a change in the dimer binding but not to a change in the reaction coordinate. Especially in polar solvents, like DMSO, DMA, and DMF, many minima are observed and it is not meaningful to directly compare these configurations. All the PMFs for dimer DA tend to extend to the region of smaller values in the reaction coordinate (Figure 6), which might reveal that the channel-type

dimer DA is less stable than DB because in most cases the layer-type dimer gives a smaller value in the reaction coordinate. Nevertheless, these results indicate clearly the relative dimer stability with and without guests in different solvents, which may provide a theoretical guidance for the preparation of CD/guest complexes in aqueous and non-aqueous phases.

CONCLUSION

In this work, we have performed molecular dynamics (MD) simulations of a β -cyclodextrin (β -CD) monomer and head-to-head dimer in 10 organic solvents to investigate orientational preferences of interglucopyranose hydrogen bonds (HBs) at the secondary rim of β -CD and the dimer binding with and without a guest molecule umbelliferone. MD results indicate that solvent properties like the HB donor and acceptor propensity, polarity, or dielectric constant can yield some qualitative insight into the HB orientation and dimer stability of CDs. Simplifications attempting to pin down solvent properties with one or two numbers are however unlikely to be good quantitative indicators of the dimer binding (Figure 8). We therefore advocate embracing the inherent complexity in processes like solvation, binding, and molecular recognition, since the corresponding energies can now be determined accurately by established simulation methods without great difficulty.

ASSOCIATED CONTENT

Supporting Information

Structural models of β -CD monomer and dimer, force field validation, structural change of free monomers in water and CHCl_3 , electrostatic interactions between monomers, and guest-induced structural change of β -CD in CHCl_3 . This material is available free of charge via the Internet at <http://pubs.acs.org>.

AUTHOR INFORMATION

Corresponding Author

*E-mail: twtan@mail.buct.edu.cn (T.T.); spoel@xray.bmc.uu.se (D.v.d.S.).

Notes

The authors declare no competing financial interest.

ACKNOWLEDGMENTS

The authors thank Dr. Daniel Larsson and Dr. Jochen Hub for PMF assistance. We acknowledge the Swedish research council for a grant of computer time (SNIC020-11-15) through the high performance computing center north (HPC2N) at Umeå Universitet and the China scholarship council (CSC) for providing a scholarship for H.Z. This research was supported by the National Natural Science Foundation of China (21076017, 20876011), 863 program (2007AA100404), and 973 program (2009CB24703, 2011CB710805).

REFERENCES

- (1) Lipkowitz, K. B. *Chem. Rev.* **1998**, *98*, 1829–1873.
- (2) Szejtli, J. *Chem. Rev.* **1998**, *98*, 1743–1753.
- (3) Jazkewitsch, O.; Mondrzyk, A.; Staffel, R.; Ritter, H. *Macromolecules* **2011**, *44*, 1365–1371.
- (4) Marcy, J. E.; Koontz, J. L.; O'Keefe, S. F.; Duncan, S. E. *J. Agric. Food Chem.* **2009**, *57*, 1162–1171.
- (5) Schneiderman, E.; Stalcup, A. M. *J. Chromatogr., B* **2000**, *745*, 83–102.

- (6) Uekama, K.; Hirayama, F.; Irie, T. *Chem. Rev.* **1998**, *98*, 2045–2076.
- (7) van de Manakker, F.; Vermonden, T.; van Nostrum, C. F.; Hennink, W. E. *Biomacromolecules* **2009**, *10*, 3157–3175.
- (8) Liu, Y.; Chen, Y. *Acc. Chem. Res.* **2006**, *39*, 681–691.
- (9) Harada, A. *Acc. Chem. Res.* **2001**, *34*, 456–464.
- (10) Paulidou, A.; Maffeo, D.; Yannakopoulou, K.; Mavridis, I. M. *CrystEngComm* **2010**, *12*, 517–525.
- (11) Brocos, P.; Díaz-Vergara, N.; Banquy, X.; Pérez-Casas, S.; Costas, M.; Piñeiro, A. n. *J. Phys. Chem. B* **2010**, *114*, 12455–12467.
- (12) Chatziefthimiou, S. D.; Yannakopoulou, K.; Mavridis, I. M. *CrystEngComm* **2007**, *9*, 976–979.
- (13) Harada, A.; Takashima, Y.; Yamaguchi, H. *Chem. Soc. Rev.* **2009**, *38*, 875–882.
- (14) Avakyan, V. G.; Nazarov, V. B.; Alfimov, M. V.; Bagaturyants, A. A.; Voronezhcheva, N. I. *Russ. Chem. Bull.* **2001**, *50*, 206–216.
- (15) Bonnet, P.; Jaime, C.; Morin-Allory, L. *J. Org. Chem.* **2001**, *66*, 689–692.
- (16) Pozuelo, J.; Mendicuti, F.; Mattice, W. L. *Macromolecules* **1997**, *30*, 3685–3690.
- (17) Liu, P.; Chipot, C.; Shao, X.; Cai, W. *J. Phys. Chem. C* **2012**, *116*, 17913–17918.
- (18) Cai, W.; Sun, T.; Shao, X.; Chipot, C. *Phys. Chem. Chem. Phys.* **2008**, *10*, 3236–43.
- (19) Naidoo, K. J.; Chen, J. Y. J.; Jansson, J. L. M.; Widmalm, G.; Maliniak, A. J. *Phys. Chem. B* **2004**, *108*, 4236–4238.
- (20) Naidoo, K. J.; Gamielien, M. R.; Chen, J. Y. J.; Widmalm, G.; Maliniak, A. J. *Phys. Chem. B* **2008**, *112*, 15151–15157.
- (21) Harada, A.; Li, J.; Kamachi, M.; Kitagawa, Y.; Katsube, Y. *Carbohydr. Res.* **1997**, *305*, 127–129.
- (22) Nascimento, C. S.; Anconi, C. P. A.; Dos Santos, H. F.; De Almeida, W. B. *J. Phys. Chem. A* **2005**, *109*, 3209–3219.
- (23) Bonnet, P.; Jaime, C.; Morin-Allory, L. *J. Org. Chem.* **2002**, *67*, 8602–8609.
- (24) Tallury, S. S.; Smyth, M. B.; Cakmak, E.; Pasquinielli, M. A. *J. Phys. Chem. B* **2012**, *116*, 2023–2030.
- (25) Jana, M.; Bandyopadhyay, S. *J. Phys. Chem. B* **2011**, *115*, 6347–6357.
- (26) Raffaini, G.; Ganazzoli, F. *J. Phys. Chem. B* **2010**, *114*, 7133–7139.
- (27) Zifferer, G.; Sellner, B.; Kornherr, A.; Krois, D.; Brinker, U. H. *J. Phys. Chem. B* **2008**, *112*, 710–714.
- (28) Zhang, H.; Feng, W.; Li, C.; Tan, T. *J. Phys. Chem. B* **2010**, *114*, 4876–4883.
- (29) Boonyarattanakalin, K. S.; Wolschann, P.; Lawtrakul, L. *J. Inclusion Phenom. Macrocyclic Chem.* **2011**, *70*, 279–290.
- (30) Zheng, X.; Wang, D.; Shuai, Z.; Zhang, X. *J. Phys. Chem. B* **2011**, *116*, 823–832.
- (31) Patey, G. N.; Valteau, J. P. *Chem. Phys. Lett.* **1973**, *21*, 297–300.
- (32) Torrie, G. M.; Valteau, J. P. *Chem. Phys. Lett.* **1974**, *28*, 578–581.
- (33) Torrie, G. M.; Valteau, J. P. *J. Comput. Phys.* **1977**, *23*, 187–199.
- (34) Lemkul, J. A.; Bevan, D. R. *J. Phys. Chem. B* **2010**, *114*, 1652–1660.
- (35) Rashid, M. H.; Kuyucak, S. *J. Phys. Chem. B* **2012**, *116*, 4812–4822.
- (36) Hub, J. S.; Winkler, F. K.; Merrick, M.; de Groot, B. L. *J. Am. Chem. Soc.* **2010**, *132*, 13251–13263.
- (37) Wennberg, C. L.; van der Spoel, D.; Hub, J. S. *J. Am. Chem. Soc.* **2012**, *134*, 5351–5361.
- (38) Zhang, Q.; Tu, Y.; Tian, H.; Zhao, Y.-L.; Stoddart, J. F.; Ågren, H. *J. Phys. Chem. B* **2010**, *114*, 6561–6566.
- (39) Coleman, C.; Hub, J. S.; van Maaren, P. J.; van der Spoel, D. *Proc. Natl. Acad. Sci. U.S.A.* **2011**, *108*, 6838–6842.
- (40) Hub, J. S.; Coleman, C.; van der Spoel, D. *Phys. Chem. Chem. Phys.* **2012**, *14*, 9537–9545.
- (41) Wang, E.; Chen, G.; Han, C. *Chin. J. Chem.* **2011**, *29*, 617–622.

- (42) de Lima, F. v. O.; Nonato, F. R.; Couto, R. D.; Barbosa Filho, J. M.; Nunes, X. P.; Ribeiro dos Santos, R.; Soares, M. B. P.; Villarreal, C. F. *J. Nat. Prod.* **2011**, *74*, 596–602.
- (43) Cezard, C.; Trivelli, X.; Aubry, F.; Djedaini-Pilard, F.; Dupradeau, F. Y. *Phys. Chem. Chem. Phys.* **2011**, *13*, 15103–15121.
- (44) Kirschner, K. N. *Proc. Natl. Acad. Sci. U.S.A.* **2001**, *98*, 10541–10545.
- (45) Basma, M.; Sundara, S.; Çalgan, D.; Vernali, T.; Woods, R. J. *J. Comput. Chem.* **2001**, *22*, 1125–1137.
- (46) Kirschner, K. N.; Woods, R. J. *J. Phys. Chem. A* **2001**, *105*, 4150–4155.
- (47) Cornell, W. D.; Cieplak, P.; Bayly, C. I.; Gould, I. R.; Merz, K. M.; Ferguson, D. M.; Spellmeyer, D. C.; Fox, T.; Caldwell, J. W.; Kollman, P. A. *J. Am. Chem. Soc.* **1995**, *117*, 5179–5197.
- (48) Case, D. A.; Darden, T. A.; Cheatham, T. E., III; Simmerling, C. L.; Wang, J.; Duke, R. E.; Luo, R.; Crowley, M.; Walker, R. C.; et al. *AMBER 10*; University of California: San Francisco, CA, 2008.
- (49) Hess, B.; Kutzner, C.; van der Spoel, D.; Lindahl, E. *J. Chem. Theory Comput.* **2008**, *4*, 435–447.
- (50) van der Spoel, D.; Lindahl, E.; Hess, B.; Groenhof, G.; Mark, A. E.; Berendsen, H. J. C. *J. Comput. Chem.* **2005**, *26*, 1701–1718.
- (51) Wang, J. M.; Wolf, R. M.; Caldwell, J. W.; Kollman, P. A.; Case, D. A. *J. Comput. Chem.* **2004**, *25*, 1157–1174.
- (52) van der Spoel, D.; van Maaren, P. J.; Caleman, C. *Bioinformatics* **2012**, *28*, 752–753.
- (53) Caleman, C.; van Maaren, P. J.; Hong, M.; Hub, J. S.; Costa, L. T.; van der Spoel, D. *J. Chem. Theory Comput.* **2011**, *8*, 61–74.
- (54) Besler, B. H.; Merz, K. M.; Kollman, P. A. *J. Comput. Chem.* **1990**, *11*, 431–439.
- (55) Jorgensen, W. L.; Chandrasekhar, J.; Madura, J. D.; Impey, R. W.; Klein, M. L. *J. Chem. Phys.* **1983**, *79*, 926–935.
- (56) Duan, Y.; Wu, C.; Chowdhury, S.; Lee, M. C.; Xiong, G. M.; Zhang, W.; Yang, R.; Cieplak, P.; Luo, R.; Lee, T.; et al. *J. Comput. Chem.* **2003**, *24*, 1999–2012.
- (57) Zhang, H.; Ge, C.; van der Spoel, D.; Feng, W.; Tan, T. *J. Phys. Chem. B* **2012**, *116*, 3880–3889.
- (58) Starr, F. W.; Nielsen, J. K.; Stanley, H. E. *Phys. Rev. E* **2000**, *62*, 579–587.
- (59) Kumar, S.; Rosenberg, J. M.; Bouzida, D.; Swendsen, R. H.; Kollman, P. A. *J. Comput. Chem.* **1992**, *13*, 1011–1021.
- (60) Hub, J. S.; de Groot, B. L.; van der Spoel, D. *J. Chem. Theory Comput.* **2010**, *6*, 3713–3720.
- (61) Abraham, M. H. *Chem. Soc. Rev.* **1993**, *22*, 73–83.
- (62) Kamlet, M. J.; Abboud, J. L. M.; Abraham, M. H.; Taft, R. W. *J. Org. Chem.* **1983**, *48*, 2877–2887.
- (63) Tetko, I. V.; Tanchuk, V. Y.; Villa, A. E. P. *J. Chem. Inf. Comput. Sci.* **2001**, *41*, 1407–1421.
- (64) Tetko, I. V.; Tanchuk, V. Y. *J. Chem. Inf. Comput. Sci.* **2002**, *42*, 1136–1145.
- (65) Betzel, C.; Saenger, W.; Hingerty, B. E.; Brown, G. M. *J. Am. Chem. Soc.* **1984**, *106*, 7545–7557.
- (66) van der Spoel, D.; van Maaren, P. J.; Larsson, P.; Timneanu, N. *J. Phys. Chem. B* **2006**, *110*, 4393–4398.
- (67) Saenger, W. *J. Inclusion Phenom. Macrocyclic Chem.* **1984**, *2*, 445–454.
- (68) Hernández, R.; Rusa, M.; Rusa, C. C.; López, D.; Mijangos, C.; Tonelli, A. E. *Macromolecules* **2004**, *37*, 9620–9625.
- (69) Bell, R. P. *Trans. Faraday Soc.* **1931**, *27*, 797–802.
- (70) Onsager, L. *J. Am. Chem. Soc.* **1936**, *58*, 1486–1493.
- (71) Yong, C. W.; Washington, C.; Smith, W. *Pharm. Res.* **2007**, *25*, 1092–1099.
- (72) Gillet, B.; Nicole, D. J.; Delpuech, J.-J. *Tetrahedron Lett.* **1982**, *23*, 65–68.
- (73) Onda, M.; Yamamoto, Y.; Inoue, Y.; Chujo, R. *Bull. Chem. Soc. Jpn.* **1988**, *61*, 4015–4021.
- (74) Anconi, C. P. A.; Nascimento, C. S.; Fedoce-Lopes, J.; Dos Santos, H. F.; De Almeida, W. B. *J. Phys. Chem. A* **2007**, *111*, 12127–12135.
- (75) van Dienst, E. v.; Snellink, B. H. M.; von Piekartz, I.; Gansey, M. H. B. G.; Venema, F.; Feiters, M. C.; Nolte, R. J. M.; Engbersen, J. F. J.; Reinhoudt, D. N. *J. Org. Chem.* **1995**, *60*, 6537–6545.
- (76) Casu, B.; Reggiani, M.; Gallo, G. G.; Vigevari, A. *Tetrahedron* **1968**, *24*, 803–821.
- (77) Kanaya, A.; Takashima, Y.; Harada, A. *J. Org. Chem.* **2010**, *76*, 492–499.
- (78) Ba, O. M.; Lahiani-Skiba, M.; Bouzbouz, S.; Skiba, M. *J. Inclusion Phenom. Macrocyclic Chem.* **2011**, *69*, 333–337.
- (79) Bicchì, C.; Cagliero, C.; Liberto, E.; Sgorbini, B.; Martina, K.; Cravotto, G.; Rubiolo, P. *J. Chromatogr. A* **2010**, *1217*, 1106–1113.
- (80) Ishimaru, Y.; Masuda, T.; Iida, T. *Tetrahedron Lett.* **1997**, *38*, 3743–3744.
- (81) Aree, T.; Chaichit, N. *Carbohydr. Res.* **2003**, *338*, 439–446.
- (82) Harata, K.; Kawano, K. *Carbohydr. Res.* **2002**, *337*, 537–547.
- (83) Coleman, A. W.; Nicolis, I.; Keller, N.; Dalbiez, J. P. *J. Inclusion Phenom. Macrocyclic Chem.* **1992**, *13*, 139–143.
- (84) Anconi, C. P. A.; Nascimento, C. S.; De Almeida, W. B.; Dos Santos, H. F. *J. Phys. Chem. B* **2009**, *113*, 9762–9769.
- (85) Dodziuk, H. *J. Mol. Struct.* **2002**, *614*, 33–45.